frontiers | Frontiers in Environmental Chemistry

TYPE Methods
PUBLISHED 01 March 2024
DOI 10.3389/fenvc.2024.1379862

OPEN ACCESS

EDITED BY
Susanta Lahiri,
Saha Institute of Nuclear Physics (SINP), India

REVIEWED BY
Gunther Korschinek,
Technical University of Munich, Germany
Timothy Jull,
University of Arizona, United States

*CORRESPONDENCE
Sebastian Fichter,
s.fichter@hzdr.de
Dominik Koll,
d.koll@hzdr.de

RECEIVED 31 January 2024
ACCEPTED 16 February 2024
PUBLISHED 01 March 2024

CITATION
Fichter S, Koll D, Rolofs A and Wallner A (2024), Case studies of three geological archives for rare radionuclide measurements using accelerator mass spectrometry.
Front. Environ. Chem. 5:1379862.
doi: 10.3389/fenvc.2024.1379862

Case studies of three geological archives for rare radionuclide measurements using accelerator mass spectrometry

Sebastian Fichter[1]*, Dominik Koll[1,2,3]*, Annabel Rolofs[1,4] and Anton Wallner[1,3]

[1]Accelerator Mass Spectrometry and Isotope Research, Helmholtz-Zentrum Dresden-Rossendorf, Dresden, Germany, [2]Department of Nuclear Physics and Accelerator Applications, The Australian National University, Canberra, ACT, Australia, [3]Institute of Nuclear and Particle Physics, Technical University Dresden, Dresden, Germany, [4]Department of Physics and Astronomy, University of Bonn, Bonn, Germany

Long-lived radionuclides in our environment provide important information on natural and anthropogenic processes. Their presence and concentration reflect the balance of production and decay. Geological archives store such information and the nuclides can be chemically extracted from the bulk sample. Accelerator mass spectrometry (AMS) represents a sensitive method to quantify those nuclides at natural levels. Three different terrestrial archives are discussed here as examples for radionuclide extraction using various chemical separation methods for subsequent AMS measurements. We focus on sample preparation for the cosmogenic radionuclides ^{10}Be and ^{26}Al, various anthropogenic actinide isotopes such as U, Pu, and Am as well as the astrophysically interesting nuclides ^{41}Ca, ^{53}Mn, and ^{60}Fe. The processed materials cover samples with masses between a few mg and up to a few hundred kg and protocols are presented for the quantitative extraction of some 10,000 atoms of cosmogenic or interstellar origin per sample and even as low as a few hundred actinide atoms.

KEYWORDS

accelerator mass spectrometry, radionuclides, environment, chemical purification, astrophysics

1 Radionuclides in the environment analysed using accelerator mass spectrometry

The concentration of rare radionuclides in our environment is an imprint of natural processes or anthropogenic activities. The detection of longer-lived radionuclides, thus, provides valuable information on our environment at large as radionuclides decay over time and their abundance is the result of the interplay of build-up and decay. The half-life of a nuclide defines the relevant time-scale of those processes that can be studied via a specific radionuclide. Longer-lived radionuclides with half-lives of 10^3 yr $< t_{1/2} < 10^8$ yr become incorporated into geological archives and, if separated from exchange with the environment, their radioactive decay can be used to date archives. None of these radionuclides have a half-life long enough for their primordial deposits to have outlasted the time since the formation of the solar system about 4.6 billion years ago (Bouvier and Wadhwa, 2010).

Today, anthropogenic radionuclides are found as a global signal through the intense nuclear weapons testing period between 1952 and 1963. Also, the nuclear activities associated with energy production (such as reactor accidents and release of radioactivity into the environment from reprocessing plants) or in medical applications imprinted an artificial isotopic signature on our environment that can be used for various environmental studies. In fact, the distinctive imprint may even define a new geological epoch, the Anthropocene. The measurement of such radionuclides with the ultrasensitive method of Accelerator Mass Spectrometry (AMS) not only allows for the study of these environmental processes and monitoring anthropogenic activities, but also paves the way for research into fundamental scientific questions.

AMS offers the potential to quantify these radionuclides as isotopic abundances (radionuclides or rare isotopes versus stable isotopes) at their natural levels, with isotopic ratios typically ranging between 10^{-10} and 10^{-16}. It represents a method to directly count and identify individual rare atoms. As such, it allows the measurement of minute amounts of radionuclides such as ^{14}C, ^{10}Be or ^{239}Pu, via their respective isotopic ratios, e.g., ^{14}C/^{12}C, ^{10}Be/^{9}Be or ^{239}Pu/^{242}Pu (Finkel and Suter, 1993; Synal, 2013; 2022; Kutschera et al., 2023). ^{12}C or ^{9}Be represent the natural elemental content via a stable isotope. In some cases, the content of the reference isotope may be too small (e.g., for ^{9}Be in seawater, see below) or, as in the case of Pu, no stable isotope exists at all. In these cases, the sample may be spiked with a quantitative amount of the reference isotope (e.g., ^{9}Be); or for Pu-AMS e.g., ^{242}Pu is an artificial tracer added to allow for isotope ratio measurements. The respective concentrations of the radionuclides (i.e., the absolute number of nuclides in a sample) can be determined from an independent measurement of the stable element concentrations (e.g., via inductively-coupled plasma mass spectrometry, ICP-MS); or in case of ^{239}Pu simply by using the well-known amount of ^{242}Pu added to the sample.

The key difference of accelerator mass spectrometry compared to conventional mass spectrometry techniques is the addition of a particle accelerator. The use of an accelerator reduces measurement background by orders of magnitude compared to techniques such as ICP-MS or secondary-ion mass spectrometry (SIMS) by providing complete background suppression of molecular isobars. In AMS, an ion beam is produced, and subsequently, the ions are separated and analysed according to their mass, particle energy, and charge state by electric and magnetic components. Rare isotopes are counted with particle detectors one by one, while the beam intensity of stable ions is measured as an electric current with Faraday cups. During the measurement the sample material is consumed slowly at consumption rates of less than or on the order of mg per measurement hour. The abundance sensitivity in AMS is limited by the overall efficiency of the rare isotope detection (this is the fraction of radionuclides in the sample that is eventually counted by the detector) but also by any residual isobaric and isotopic interferences in the detector mimicking a rare radionuclide detector signal.

AMS represents the most sensitive technique for quantifying radionuclides with half-lives 10^3 yr $< t_{1/2} < 10^8$ yr in the environment and enables a wide range of applications (Kutschera et al., 2023). Before an AMS measurement takes place, the isotopes of interest must be separated from the original matrix by dedicated chemical procedures to reduce the sample matrix by orders of magnitude and to purify the desired elemental fractions. In the following, the search for rare radionuclides in three different geological archives is presented with regards to the potential field of application in climate and environmental research as well as nuclear astrophysics. Chemical reagents as well as ultra-pure water must be devoid of both the respective radionuclide and its stable isotope. This is regularly the case for water purification systems and most commercially available reagents, however, radionuclides such as ^{10}Be, ^{36}Cl or ^{129}I might require pre-screening of the chemicals used (Merchel et al., 2021; Fifield et al., 2022).

2 Geological samples

2.1 Case 1: deep-ocean ferromanganese crusts (^{10}Be, ^{26}Al)

Deep-ocean ferromanganese (Fe/Mn) crusts are slow-growing metallic underwater rocks found in all major oceans on Earth (Hein and Koschinsky, 2014). The growth of the here considered class of Fe/Mn crusts is induced by hydrogenetic precipitation of vernadite and feroxyhyte out of seawater onto a sediment-free rock substrate (Koschinsky and Halbach, 1995; Halbach et al., 2017). Typical growth-rates of Fe/Mn crusts are on the order of mm/Myr. This allows to investigate Earth's history for interstellar radionuclide influxes (Knie et al., 1999; 2004; Wallner et al., 2015; 2016; 2021; Koll, 2023) on a Myr timescale in addition to deep-ocean sediments (Fitoussi et al., 2008; Ludwig et al., 2016; Wallner et al., 2016; 2020) and Antarctic ice and snow (Koll et al., 2019). Fe/Mn crusts are rich in rare-earth elements as well as in Ni and in particular Co (0.2–2%), leading to their similarly common name Co-rich Fe/Mn crusts and making them an important resource for future industrial mining (Halbach et al., 2017).

The radioactive decay of incorporated ^{10}Be ($t_{1/2}$ = 1.39 Myr, Korschinek et al., 2010; Chmeleff et al., 2010) is most commonly used to date Fe/Mn crusts and to determine their growth-rate. Cosmogenic ^{10}Be is produced in the upper atmosphere by galactic cosmic rays striking nitrogen and oxygen molecules, breaking the nuclides up and forming the spallation product ^{10}Be (Masarik and Beer, 1999). A steady cosmic ray flux and composition of the atmosphere lead to a relatively constant production of ^{10}Be over geological timescales (Ku et al., 1982; Smith et al., 2019). The freshly produced ^{10}Be is continuously incorporated into Fe/Mn crusts. The decay of ^{10}Be can then be used as a radioactive clock to date the Fe/Mn crust, if the incorporation of Be into the crust stays constant over time. Several studies indicate a good constancy of Be incorporation in several different Fe/Mn crusts over the last 10 Myr (Bourles et al., 1989; Segl et al., 1984; Koll and Lachner, 2023; von Blanckenburg et al., 1996b). Differences in Be uptake in deep-ocean sediments were assigned to varying Ca concentrations in them (Feige, 2014). The Ca content of Fe/Mn crusts is low and constant and does, therefore, not influence the Be uptake (Koll, 2023).

The production rate of ^{10}Be in the upper atmosphere of $\approx 6 \times 10^5$ at/cm^2/yr (Masarik and Beer, 1999; Nagai et al., 2000; Webber and Higbie, 2003) and the ^{9}Be concentration in sea water of $\approx 6 \times 10^{-6}$ mg/L (Haynes et al., 2014) lead to isotopic ratios of ^{10}Be/^{9}Be $\approx 10^{-7}$ in sea water and, hence, in Fe/Mn crusts.

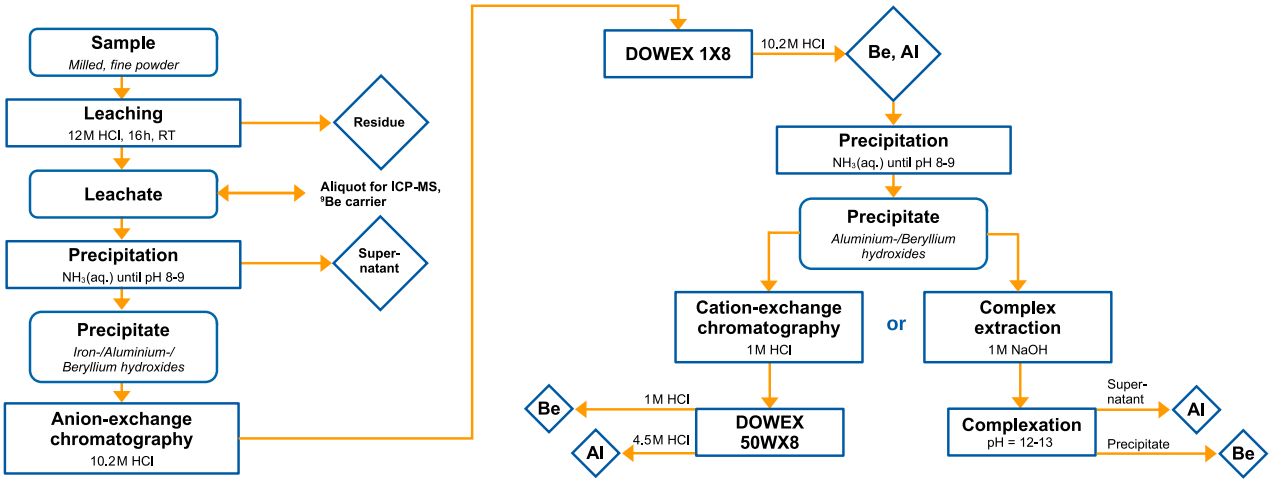

FIGURE 1
Flow chart of chemical work-up procedure for ^{10}Be and ^{26}Al extraction from 10–100 mg Fe/Mn crust. RT: room temperature.

This intrinsic ratio is several orders of magnitude higher than the sensitivity of AMS of 10^{-16}. However, the ^{9}Be concentration in Fe/Mn crusts is only a few ppm (von Blanckenburg et al., 1996a), leading to less than micrograms of ^{9}Be for the final AMS sample. Due to the high intrinsic ratio, either a carrier-free approach can be chosen, where < μg Be are extracted and dispersed in Fe carrier (Maden et al., 2004; Horiuchi and Matsuzaki, 2015; Lachner et al., 2020), or, more commonly, a known amount of ^{9}Be carrier is added to the sample (Fitoussi et al., 2008; Koll et al., 2022b). The measured ^{10}Be/^{9}Be ratio, critical for AMS, is only reduced by a few orders of magnitude compared to the intrinsic ratio through carrier addition and still easily measurable by AMS.

The chemical extraction of Be and several other elements from Fe/Mn crusts was described in detail by Koll et al. (2022b) and Koll (2023). Here, the chemistry protocol is described with a focus on Be and more recent findings. A schematic summary of the procedure can be found in Figure 1.

Beryllium is extracted from 10–100 mg of milled Fe/Mn crust powder by first dissolving the powder in 15 mL of 10.2 M HCl and 0.25 mL of 30% H_2O_2 at room temperature. Seawater beryllium, and therefore, atmospheric ^{10}Be that were incorporated in the leachable part of the Fe/Mn matrix are dissolved. Any unwanted *in-situ* produced ^{10}Be as well as terrestrial Be in the insoluble mineral fraction of silicates and zircons are discarded. The dissolved Be is precipitated together with Fe, Al, and Ti hydroxides by the addition of NH_3(aq.) until pH = 8–9. Both, Mn and Co, can either partially or not precipitate due to its oxidation state ambivalence or the formation of an ammine-complex, respectively. Abundant elements such as Na, Mg or Ca do not form insoluble hydroxides at this pH and stay in the supernatant. The most important isobaric element for ^{10}Be AMS, B, is present as anionic borate in solution and similarly separated. The pre-concentrated and purified precipitate is redissolved in 10.2 M HCl and charged to a 12 mL anion-exchange column (DOWEX 1X8). Iron is strongly retained on the column in contrast to Be, Al and Ti. After the column chromatography, the solution containing Be, Al and Ti is precipitated again by the addition of NH_3(aq.). The precipitate can directly be transformed into an AMS target by igniting it at 900°C since the Al and Ti contents are low and do not interfere with the ^{10}Be AMS measurement. In case an isolated Al fraction is required, a cation-exchange column or a complexation at pH = 12–13 (Ochs and Ivy-Ochs, 1997) can be added to separate Al from Be (see Figure 1 and Subsection 2.3.2).

It is advantageous that the final AMS target contains both fractions, Be and Al, because ^{10}Be and ^{26}Al are highly desired AMS radionuclides (see e.g., Nishiizumi et al., 1986; Granger, 2006). The measurement of both radionuclides from the same target would improve the sample throughput significantly. Typically, a good performance of Al targets with respect to ion beam current output is more critical than for Be due to the lower ^{26}Al concentration and worse negative ion formation efficiency in the sputter ion source. Therefore, a combined sample should be optimised for Al AMS. First tests, where the combined sample of BeO and Al_2O_3 was split into two and prepared as an individual Be-optimised target (mixed 1:4 wt/wt with Nb) and as an Al-optimised target (mixed 1:1 wt/wt with Ag) showed that both targets performed well in their respective radionuclide measurement. The next step is to optimise the sample preparation such that both measurements for ^{10}Be and ^{26}Al perform well from the same AMS target.

The ^{10}Be AMS technique to determine a Fe/Mn crust's growth rate is well-established and the methodology at the DREsden Accelerator Mass Spectrometry (DREAMS) facility (Akhmadaliev et al., 2013; Rugel et al., 2016; Lachner et al., 2023) will be briefly explained. The prepared BeO target (mixed with Nb, 1:4 wt/wt) is inserted into the negative ion source. After sputtering, ^{9,10}BeO^{-} is selected and injected into the accelerator where electrons are stripped and molecules dissociate. The positively charged ^{9,10}Be ions are then selected after the accelerator and guided to the detector. Interfering ^{10}B is separated from ^{10}Be by differential energy loss in a SiN foil and the subsequent passage of an electrostatic analyser. Macroscopic currents of ^{9}Be are measured in offset Faraday cups. Isotopic ratios of processed crust surface samples with previously added Be carrier are in the range of ^{10}Be/^{9}Be = 10^{-10}–10^{-11}. At the DREAMS facility, dating of ferromanganese

TABLE 1 Expected atomic ratios of actinide isotopes relative to ^{239}Pu for the global averaged nuclear fallout signal and Chernobyl debris. ^{241}Pu/^{239}Pu isotopic ratio decay corrected to 01.01.2024. Data taken from (a) Hain et al. (2020), (b) Ketterer et al. (2013), (c) UNSCEAR (2000), (d) Kelley et al. (1999), (e) Muramatsu et al. (2000), (f) Ketterer et al. (2004) and (g) Steier et al. (2013).

Atom ratio	Averaged global fallout signal	Chernobyl
^{233}U/^{236}U	$(1.4 \pm 0.2) \times 10^{-2}$ (a)	$(1.2 \pm 0.1) \times 10^{-3}$ (a)
^{236}U/^{239}Pu	$(1.9 \pm 0.4) \times 10^{-1}$ (b)	8.7 (c)
^{237}Np/^{239}Pu	$(4.1 \pm 1.0) \times 10^{-1}$ (d)	2.4×10^{-2} (c)
^{240}Pu/^{239}Pu	$(1.8 \pm 0.2) \times 10^{-1}$ (d)	$(4.0 \pm 0.2) \times 10^{-1}$ (e)
^{241}Pu/^{239}Pu	$(6.3 \pm 1.0) \times 10^{-4}$ (d)	$(2.2 \pm 0.2) \times 10^{-2}$ (f)
^{242}Pu/^{239}Pu	$(4.0 \pm 1.0) \times 10^{-3}$ (d)	$(3.4 \pm 0.2) \times 10^{-2}$ (f)
^{244}Pu/^{239}Pu	$(5.7 \pm 1.0) \times 10^{-5}$ (g)	—

crusts beyond 15 Myr is possible with high precision. Recently, a piece of the Fe/Mn crust VA13/2-237KD was ^{10}Be-dated at the DREAMS facility till 18 Myr for the search of supernova-produced ^{60}Fe and *r*-process ^{244}Pu (Koll et al., 2022b; Koll, 2023).

2.2 Case 2: urban soil (U, Pu, Am)

Atmospheric nuclear weapons test during the 1950s and 60s released huge amounts of actinides (e.g., U, Np, Pu, Am) and fission products (e.g., ^{90}Sr, ^{99}Tc, ^{129}I, ^{137}Cs) into the environment (UNSCEAR, 2010). These nuclides have spread globally and can be found on Earth's surface in oceans, soils, sediments and plants. Furthermore, major nuclear accidents as happened in Chernobyl (1986) or Fukushima-Daichi (2011) contributed to the anthropogenic radionuclide signal in the environment (NEA/OECD, 2002; Onda et al., 2020). Additionally, local sources from nuclear facilities such as nuclear power plants, reprocessing or fuel production sites could be present. The isotopic signature of actinides in environmental samples gives the unique opportunity to distinguish different sources and is essential for nuclear safeguards and non-proliferation purposes. Thus, several actinide isotopes are of interest due to their different production pathways and hence their ability to account for various sources.

Many studies focused on the isotopic ratio of the plutonium isotopes ^{240}Pu/^{239}Pu, which is only accessible with mass spectrometric techniques due to the similar α energies of both nuclides (Kelley et al., 1999). Although the Pu isotopes with higher mass numbers (i.e., ^{241}Pu, ^{242}Pu and ^{244}Pu) are produced in much lower quantities, their assessment holds potential for a deeper understanding of the source of Pu in the environment (Steier et al., 2013). Especially the shorter-lived ^{241}Pu ($t_{1/2}$ = 14.3 years) and its daughter ^{241}Am may be used for dating the last chemical separation of both elements or the date of irradiation (Steier et al., 2013; Corcho Alvarado et al., 2022. In recent years, the rare uranium isotopes ^{233}U and ^{236}U and their atomic ratio have gained much attention, especially looking in ocean water and sediments worldwide (Hain et al., 2020; Lin et al., 2021; Qiao et al., 2022).

A compilation of expected isotope ratios for global nuclear fallout in comparison to measurements from the Chernobyl debris can be found in Table 1. Within this work we present our chemical work-up protocol for the determination of actinides (i.e., U, Pu, Am) from different environmental samples like soil, sediments or plant material. The required sample size strongly depends on the isotopes to be investigated. Several studies reported the concentration of ^{239}Pu of anthropogenic origin for top soil layers in the order of 50–500 fg/g (Harley, 1980; Kelley et al., 1999; Muramatsu et al., 2000; Tighe et al., 2021). This corresponds to 10^8–10^9 atoms ^{239}Pu/g soil (1 fg Pu $\hat{=}$ 2.5×10^6 atoms Pu). As shown in Table 1 all other relevant actinide isotopes are present in smaller amounts compared to ^{239}Pu. However, state-of-the-art AMS facilities dedicated for actinide measurements reach detection efficiencies of 1% and more (Hotchkis et al., 2019; Koll et al., 2022a; Koll, 2023) enabling routine analysis of gram-sized soil samples even for less-abundant isotopes like ^{233}U and ^{244}Pu.

As already introduced in Section 1, AMS is an ultra-trace analytical method measuring isotopic ratios between rare and abundant isotopes with high sensitivity. In the case of actinides there are no abundant isotopes present in nature despite the long-lived ^{232}Th and ^{235,238}U and their daughter nuclides. Thus, for determining the content of the rare uranium isotopes ^{233}U and ^{236}U, the concentration of the primordial uranium can be analysed with less sensitive analytical methods like ICP-MS. However, the measurement of transuranium elements requires the addition of a (preferably mono-isotopic) spike of known quantity as a reference. For plutonium determination, different isotopes can be added as tracers (i.e., ^{236}Pu, ^{242}Pu or ^{244}Pu). Isotopic purity, availability and interference with other nuclides are the major factors for selecting an appropriate isotopic spike. For many actinides the limited number of long-lived and readily accessible isotopes prevents the use of an isotopic spike. Instead, neighbouring elements may be used as non-isotopic spikes (e.g., ^{243}Am as spike for ^{247}Cm or ^{242}Pu for ^{237}Np). The prerequisite for using non-isotopic spikes is a similar chemical behavior during sample preparation and a well-characterised standard material to correct the AMS measurement for differences in their ionisation efficiency and transmission through the accelerator.

The general work-up scheme for different environmental samples is shown in Figure 2. Commonly, the samples are first dried in a drying cabinet at 95°C to constant mass content. Subsequently, larger grains are removed by sieving (2 mm). Afterwards, the samples are weighed and ashed in a muffle furnace at 550°C for 5 h in order to destroy all organic materials

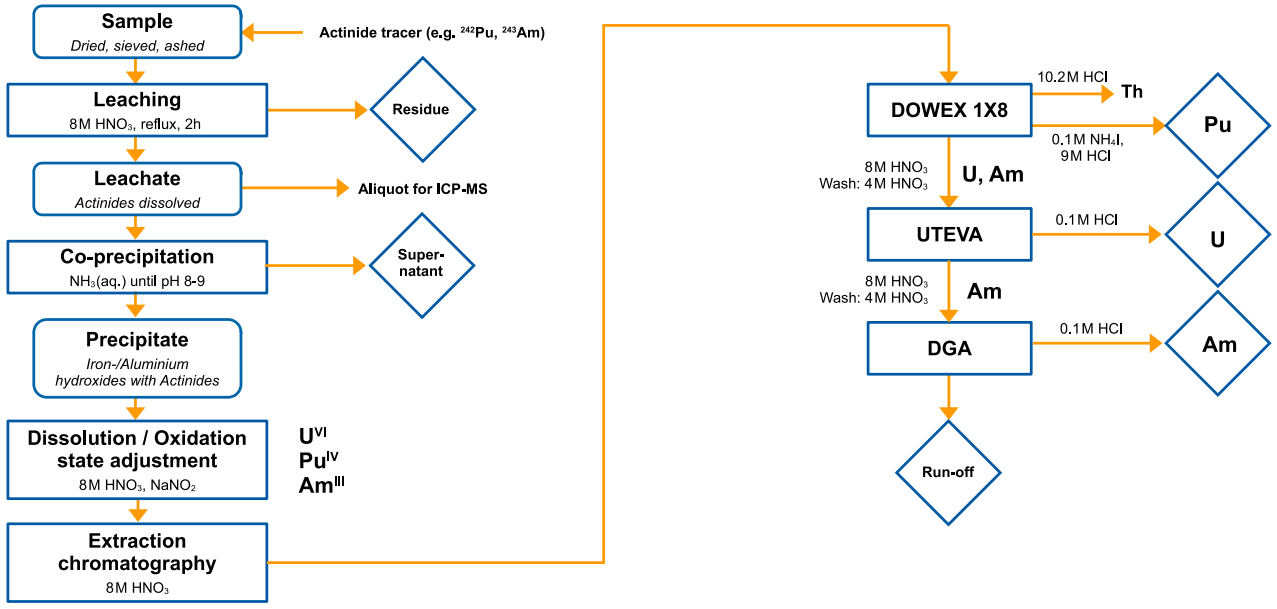

FIGURE 2
Flow chart of chemical work-up procedure for U, Pu and Am extraction from 1–5 g urban soil.

present and determine the loss-on-ignition. After ashing the residues are leached in 10 mL 8 M HNO_3 per gram sample for 2 h under reflux conditions. Although this acid leaching process does not dissolve the whole sample (silicates, zircons and refractory oxides remain) it has been shown that the majority of the targeted anthropogenic actinides are accessible (Krey and Bogen, 1987).

The separation of the actinides from the bulk sample is done by means of chemical purification steps like co-precipitation and column chromatography. For environmental samples we perform a co-precipitation of the actinides with Fe and Al hydroxides by raising the pH of the acidified solutions from leaching to pH = 8–9 with diluted NH_3(aq.). The alkali and earth-alkali metals, with the valuable exception of Be, do not form hydroxide precipitates at these pH-values and stay in the supernatant. High concentrations of iron(III) can subsequently be removed by dissolving the precipitate in 7 M hydrochloric acid and liquid-liquid extraction with diisopropyl ether. Another major constituent of soil, Al, can be decreased by making use of it's amphoteric character, forming soluble hydroxide complexes $[Al(OH)_4]^-$ at pH > 12. Generally, less matrix material facilitates a smooth column chromatography setup and avoids column blockage.

Prior to separation of the actinides from the sample using column chromatography, their oxidation state has to be adjusted. Under the given oxidising conditions in diluted nitric acid medium, uranium exclusively exists as U(VI) and americium as Am(III). Hence, only the oxidation state of Pu needs to be adjusted to Pu(IV) in order to separate the most relevant actinides according to their oxidation state and their connected chemical behavior. Addition of solid $NaNO_2$ and boiling for 30 min is sufficient for this purpose (Koll et al., 2022a).

In general, Pu is extracted from the remaining matrix as $[Pu^{IV}(NO_3)_6]^{2-}$ complex on anion exchange resin DOWEX 1X8, U as phosphonate complex on UTEVA resin and finally Am as TODGA complex on DGA resin. Hence, a stacked three column approach is used to sequentially extract the actinides of interest. After sample loading, the columns are washed with 8 M and 4 M HNO_3 to remove matrix elements (e.g., Al, Fe, Mn). Thereafter the columns are separated and treated differently to finally obtain pure fractions of the actinides. The anion exchange column is subsequently washed with 10.2 M HCl to remove the coextracted Th. Finally, Pu is eluted by reducing it to its trivalent oxidation state with 0.1 M NH_4I - 9 M HCl. Evaporation of the solution and fuming with HNO_3 and HCl destroys the remaining ammonium iodide. U and Am can be eluted from UTEVA resp. DGA columns by 0.1 M HCl.

The final AMS target preparation is similar for all separated actinides which are subsequently either co-precipitated with iron as iron(III)-hydroxides or dissolved in HNO_3 acidic iron solution and dried. The dried residues are transferred to quartz crucibles which are calcined in a muffle furnace at 600°C for 2 h to form Fe_2O_3 with embedded actinides. The resulting iron oxide powder is mixed with metal powders (e.g., Ag, Nb) and pressed into cathodes for sputtering in negative ion sources. Nowadays, actinides are more efficiently measured at compact AMS systems Vockenhuber et al., 2013; Hotchkis et al., 2019; Steier et al., 2019. Here, we exemplify the AMS setup for the two AMS facilities Vega (ANSTO) and VERA (Univ. of Vienna). For plutonium measurements at ANSTO (Wilcken et al., 2015; Hotchkis et al., 2019), mixtures of Fe_2O_3: Nb (1:1 wt/wt) are pressed into aluminium target holders. Negatively charged PuO^- ions are extracted and accelerated by setting the terminal voltage to 0.86 MV. On the high-energy side Pu^{3+} ions are counted in a gas-ionization chamber. Fast isotope cycling is applied to the low- and high-energy magnets to inject up to 8 masses of different isotopes quasi-simultaneously (Hotchkis et al., 2019). For actinide (An) measurements at the VERA facility (Steier et al., 2019; Hain et al., 2020) the iron oxide material is mixed with

silver in 1:1 weight ratio. Again, AnO^- ions are extracted and stripped to An^{3+} ions in the accelerator using 1.65 MV terminal voltage.

2.3 Case 3: Antarctic ice (^{10}Be, ^{26}Al, ^{41}Ca, ^{53}Mn and ^{60}Fe)

Stars freshly synthesise chemical elements in their interior by nuclear reactions. The life cycle of massive stars concludes with a stellar explosion, a supernova, that is ejecting most of the stars material into space, including freshly produced radionuclides. While the solar system traverses the interstellar medium, it captures interstellar dust containing live radionuclides from former supernovae (Ellis et al., 1996; Athanassiadou and Fields, 2011). These dust particles can accumulate on Earth over millions of years, leaving their isotopic fingerprints in terrestrial archives to be uncovered.

Latest endeavours focus on establishing a new geological archive for nuclear astrophysics—the ice of Antarctica. Antarctic ice serves as a unique geological reservoir for the study of extraterrestrial material due to its isolated location and the climatic conditions that preserve materials chronologically over millennia. In this project, we analyse radionuclide concentrations in continuous-flow analysis (CFA) water, extracted from an Antarctic ice core. The ice core is sourced from a drilling site near the Kohnen Station in Dronning Maud Land, Antarctica.

Our objective is to investigate an ongoing interstellar ^{60}Fe ($t_{1/2}$ = 2.6 Myr, Rugel et al., 2009; Wallner et al., 2015) influx by covering a time period between 50,000 and 80,000 years ago. Earlier studies showed ^{60}Fe activity about 2–3 Myr ago (Knie et al., 2004; Ludwig et al., 2016; Wallner et al., 2016; 2021; Koll, 2023), as well as an older influx 7–8 Myr ago (Wallner et al., 2016; 2021; Koll, 2023), both of which are attributed to interstellar dust containing traces of supernova-produced ^{60}Fe. Furthermore, a recent interstellar ^{60}Fe influx was discovered in Antarctic surface snow (Koll et al., 2019) and independently in deep-sea sediments covering the past 35 kyr (Wallner et al., 2020). A study of Antarctic ice for ^{60}Fe will, therefore, yield time-resolved data between the previously investigated timescales (Koll et al., 2020). In addition to ^{60}Fe, the atmospheric radionuclides ^{10}Be and ^{26}Al are used to characterise the Antarctic ice sample further, whereas the interplanetary isotopes ^{41}Ca and ^{53}Mn are utilised to distinctively differentiate interstellar ^{60}Fe from cosmic-ray produced ^{60}Fe (Koll et al., 2022a).

The rarity of the influx and deposition of interstellar radionuclides onto Earth constrains the usability of potential environmental archives. In order to clearly detect ^{60}Fe, a minimum of 25,000 atoms of ^{60}Fe must be present in a sample in order to obtain 10 detector events at the Heavy-Ion Accelerator Facility (HIAF) at the Australian National University (Wallner et al., 2023). Furthermore, the atomic ratio ^{60}Fe/Fe must exceed 2×10^{-16}, which is 10 times the lowest blank level. Addressing the first condition, we consider the known recent ^{60}Fe deposition rate in Antarctica of 1 at/cm^2/yr (Koll et al., 2019) and the pre-industrial accumulation rate of 66 mm w.e. yr^{-1} (Oerter et al., 2000; Birnbaum et al., 2006; Medley et al., 2018). A minimum of 165 kg of Antarctic ice is necessary to contain the required 25,000 ^{60}Fe atoms. A typical terrestrial Fe flux of 1 mg/m^2/yr (Conway et al., 2015), yields 2.5 mg of Fe in 165 kg of Antarctic ice. This results in a ratio of ^{60}Fe/Fe = 9×10^{-16}, thereby fulfilling the second condition. A higher accumulation rate of 110–250 mm w.e. yr^{-1} (Karlsson et al., 2016) and an up to 20 times higher iron content (Xiao et al., 2020) in Greenland ice would lead to a reduction of the ^{60}Fe/Fe ratio beyond detectability, primarily driven by the higher stable iron content.

The relatively low accumulation rates in Dronning Maud Land, however, still require high sample volumes to reach the sensitivity required to detect a few single atoms from an interstellar dust influx. Additionally, a chemically pure sample is essential to prevent a dilution in the Fe concentration. The chemical procedure to extract the aforementioned radionuclides from such large ice samples is based on the established procedure for a deep-ocean ferromanganese crust (Koll et al., 2022b) and meteorites (Merchel and Herpers, 1999). It is an update to the previously employed procedure for Antarctic snow (Koll, 2018; Koll et al., 2019). The chemical protocol is depicted in the flowchart in Figure 3.

A total of 300 kg of CFA water is acidified to pH = 2 by adding HNO_3 to prevent microbial contamination and ensure sample stability. An aliquot of the total volume is analysed by ICP-MS for already dissolved elements. The volume is then significantly reduced through evaporation over three to 4 weeks in two insulated and covered 10 L glass beakers under temperature-controlled conditions at 80–90 °C to prevent boiling. A 10 L blank sample from purified (18 MΩ) water is placed next to the beakers to monitor the introduction of contaminants. The progressing evaporation gradually increases the acid concentration of the sample, prompting repeated checks of the element concentrations by ICP-MS until the sample reaches 50 mL. The increasing acid concentration continuously leaches terrestrial elements from solid particles in the sample. If necessary, a filtration step could be included to restrict further leaching at the expense of potential radionuclide losses. Here, the low stable element concentrations did not require filtration even in concentrated HNO_3. The addition of H_2O_2 reduces any Mn(IV) to soluble Mn(II) in HNO_3. After evaporation, a final aliquot from the remaining 50 mL sample is taken for stable element determination before carrier solutions are added to the sample and the blank. The low natural concentrations of Be and Mn in Antarctic ice (Koll, 2018) require the addition of 2 mg Be and 3 mg Mn, whereas natural Al, Ca and Fe concentrations are high enough for carrier-free chemistry of the Antarctic ice sample. The typically added Be carrier mass in AMS is in the range of 200–500 μg, but here, this large natural sample with a considerable atmospheric ^{10}Be concentration requires further dilution to reduce the expected ^{10}Be/^{9}Be ratio.

2.3.1 Be, Al, Fe

The elements Be, Al and Fe are separated from Ca and Mn by hydroxide precipitation at pH = 8 – 9 through the addition of NH_3(aq.). This also separates the isobaric interferences ^{10}B and ^{60}Ni from the respective radionuclide of interest. The precipitate containing Be, Al and Fe is redissolved in 10.2 M HCl and loaded onto a 12 mL anion-exchange column (DOWEX 1X8), where Be and Al are passed, but Fe is retained on the column. Iron is eluted by the addition of 27.5 mL H_2O. The Be/Al fraction and the Fe fraction are precipitated again by the addition of NH_3(aq.) at pH = 8–9. The iron hydroxide is then dried and ignited at 600°C to form Fe_2O_3.

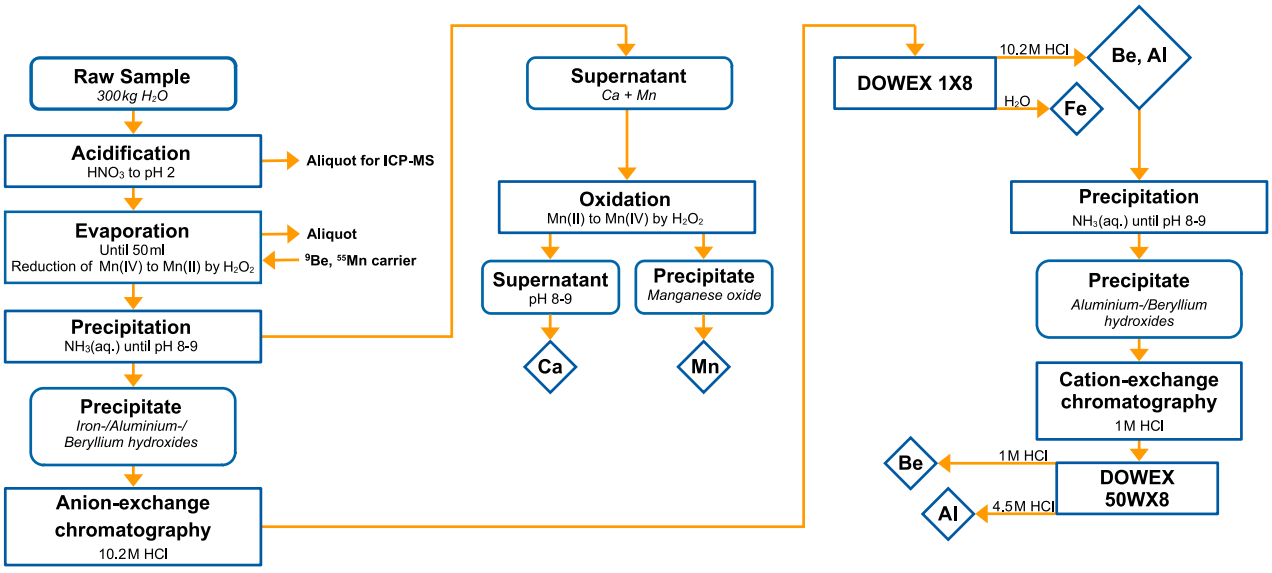

FIGURE 3
Flow chart of chemical work-up procedure for ^{10}Be, ^{26}Al, ^{41}Ca, ^{53}Mn and ^{60}Fe extraction from 300 kg Antarctic ice.

2.3.2 Be, Al

The Be/Al hydroxide is redissolved in 1 M HCl and charged to a 12 mL cation-exchange column (DOWEX 50WX8) to separate Be from retained Al. Residual B is separated from Be by addition of 35 mL 1 M HCl, followed by 110 mL 1 M HCl for Be elution. The addition of 47.5 mL 4.5 M HCl finally elutes Al. This column separation is repeated due to the high concentration of Al in this sample to obtain pure Be and Al fractions. A complexation approach at pH = 12–13 (Ochs and Ivy-Ochs, 1997) is less preferable due to the large quantities of natural Al in this particular sample. The separated Be and Al fraction are precipitated by the addition of NH_3(aq.) until pH = 8–9. Both, Be and Al hydroxides, are dried and then ignited at 900°C for 2 h to form Al_2O_3 and BeO, respectively.

2.3.3 Mn

To isolate Mn from the supernatant that contains the dissolved Ca and Mn, H_2O_2 is added to oxidise Mn(II) to MnO_2, which precipitates out of solution. The AMS of ^{53}Mn requires a further purification from its isobar ^{53}Cr by a $KClO_3$ precipitation in small volumes. The redissolved Mn fraction is placed on a hot plate in 10 mL concentrated HNO_3, to which potassium chlorate is added sequentially until the precipitation of MnO_2 as brown precipitate is observed. This purification step is repeated twice to ensure the lowest Cr levels necessary for ^{53}Mn AMS measurements. The purified MnO_2 is dried at 90°C in a drying cabinet for 72 h.

2.3.4 Ca

The Ca fraction is further processed in three consecutive precipitation steps. First, Ca is separated from Mg by precipitation as hydroxide with 1 M NaOH at pH = 10–11. $(NH_4)_2C_2O_4$ selectively precipitates Ca as CaC_2O_4. Taking advantage of the fact that ammonium oxalate is more soluble at higher temperatures, the Ca sample is precipitated in warm conditions. This is followed by a CaF_2 precipitation in 3 mL 4 M HNO_3 and addition of 1 mL 48% HF. Lastly, CaF_2 is dried at 70°C overnight.

2.3.5 AMS targets

The final samples are prepared as AMS targets by mixing them with metal powders: BeO (1:4 wt/wt with Nb), Al_2O_3 (1:1 wt/wt with Ag), CaF_2 (1:4 wt/wt with Ag), MnO_2 (1:1 wt/wt with Cr-reduced Ag powder) and Fe_2O_3 (1:1 wt/wt with Ag) and then pressed into Cu cathodes. The radionuclides ^{10}Be, ^{26}Al and ^{41}Ca are measured at the DREAMS facility (Akhmadaliev et al., 2013; Lachner et al., 2023; Vivo-Vilches et al., 2023), while ^{53}Mn and ^{60}Fe are measured at HIAF (Wallner et al., 2023).

3 Summary

Accelerator mass spectrometry has proven to be a versatile tool for the detection of rare radionuclides. It offers a dynamical range in abundance ratios over several orders of magnitude and detection sensitivities are approaching a few hundred atoms per sample for some nuclides. However, even at these ultra-low detection limits, the measurement of certain radionuclides, especially of extraterrestrial origin, still require large sample sizes. Using production rates, deposition and incorporation efficiencies of some radionuclides, we calculated above the relevant sample sizes for three different cases to enable their detection with AMS. Proper chemical treatment strategies are indispensable to extract and separate radionuclides out of a large sample matrix. The case studies presented show the chemical work-up protocol for determining cosmogenic ^{10}Be and ^{26}Al from 10–100 mg Fe/Mn crust, anthropogenic U, Pu and Am isotopes from 1–5 g of urban soil and extraterrestrial ^{41}Ca, ^{53}Mn and ^{60}Fe from 300 kg of Antarctic ice. In all chemical treatment strategies hydroxide precipitation out of acidified solutions is the first step to separate high-valent cations which are forming sparingly soluble hydroxide precipitates (i.e., Al, Fe, Ti, Be and actinides) from mono- and divalent

cations (i.e., Na, K, Mg, Ca, Mn, Ni) which stay in the supernatant at pH = 8–9. Subsequently, different complex formation tendencies of metal cations are used to separate them using anion- and cation-exchange columns (DOWEX 1X8 and DOWEX 50WX8) and extraction chromatography with organic ligands impregnated onto an inert support (UTEVA and DGA resin from Triskem for actinide separation). Finally, AMS targets are prepared by embedding the radionuclides into a stable inorganic oxide or fluoride matrix consisting of the stable reference nuclide or, in the case of actinides, into iron(III) oxide. These chemical treatment strategies are not limited to the presented sample types and can be easily adapted and scaled to new projects. In addition to such optimised chemical separation strategies, also the recent technological progress made in rare isotope detection, as, e.g., implemented at the new AMS facility HAMSTER (*Helmholtz Accelerator Mass Spectrometer Tracing Environmental Radionuclides*) at HZDR, will further improve measurement sensitivities. Consequently, AMS represents an important tool to address open questions in climate research, Earth science or in astrophysics, but also for studying the anthropogenic environmental impact.

Data availability statement

The original contributions presented in the study are included in the article/Supplementary material, further inquiries can be directed to the corresponding authors.

Author contributions

SF: Conceptualization, Methodology, Writing–original draft, Writing–review and editing, Funding acquisition. DK: Conceptualization, Methodology, Writing–original draft, Writing–review and editing, Funding acquisition. AR: Writing–original draft, Writing–review and editing, Methodology. AW: Funding acquisition, Methodology, Project administration, Writing–original draft, Writing–review and editing.

Funding

The author(s) declare that financial support was received for the research, authorship, and/or publication of this article. DK was supported by an AINSE Ltd. Postgraduate Research Award (PGRA). The AMS measurements were funded through the RADIATE project from the EU Research and Innovation program HORIZON 2020, project numbers 21002421-ST, 20002142-ST, 22003021-ST and 22003093-ST, the Ion Beam Center of HZDR, project numbers 22002913-EF, 22003072-EF and 23003438-ST and the National Collaborative Research Infrastructure Strategy (NCRIS) of the Australian Government.

Acknowledgments

The authors want to express their gratitude to Florian Adolphi and Maria Hoerhold for providing the Antarctic ice sample and valuable input. Karin Hain and Peter Steier from VERA are gratefully acknowledged for performing actinide AMS measurements.

Conflict of interest

The authors declare that the research was conducted in the absence of any commercial or financial relationships that could be construed as a potential conflict of interest.

Publisher's note

References

Akhmadaliev, S., Heller, R., Hanf, D., Rugel, G., and Merchel, S. (2013). The new 6MV AMS-facility DREAMS at Dresden. *Nucl. Instrum. Methods Phys. Res. Sect. B Beam Interact. Mater. Atoms* 294, 5–10. doi:10.1016/j.nimb.2012.01.053

Athanassiadou, T., and Fields, B. (2011). Penetration of nearby supernova dust in the inner solar system. *New Astron.* 16, 229–241. doi:10.1016/j.newast.2010.09.007

Birnbaum, G., Brauner, R., and Ries, H. (2006). Synoptic situations causing high precipitation rates on the Antarctic plateau: observations from Kohnen Station, Dronning Maud Land. *Antarct. Sci.* 18, 279–288. doi:10.1017/S0954102006000320

Bourles, D., Raisbeck, G., and Yiou, F. (1989). ^{10}Be and ^{9}Be in marine sediments and their potential for dating. *Geochimica Cosmochimica Acta* 53, 443–452. doi:10.1016/0016-7037(89)90395-5

Bouvier, A., and Wadhwa, M. (2010). The age of the solar system redefined by the oldest Pb–Pb age of a meteoritic inclusion. *Nat. Geosci.* 3, 637–641. doi:10.1038/ngeo941

Chmeleff, J., von Blanckenburg, F., Kossert, K., and Jakob, D. (2010). Determination of the ^{10}Be half-life by multicollector ICP-MS and liquid scintillation counting. *Nucl. Instrum. Methods Phys. Res. Sect. B Beam Interact. Mater. Atoms* 268, 192–199. doi:10.1016/j.nimb.2009.09.012

Conway, T. M., Wolff, E. W., Röthlisberger, R., Mulvaney, R., and Elderfield, H. (2015). Constraints on soluble aerosol iron flux to the southern ocean at the last glacial maximum. *Nat. Commun.* 6, 7850. doi:10.1038/ncomms8850

Corcho Alvarado, J. A., Röllin, S., Sahli, H., and McGinnity, P. (2022). Isotopic signatures of plutonium and uranium at Bikar Atoll, northern Marshall Islands. *J. Environ. Radioact.* 242, 106795. doi:10.1016/j.jenvrad.2021.106795

Ellis, J., Fields, B. D., and Schramm, D. N. (1996). Geological isotope anomalies as signatures of nearby supernovae. *Astrophysical J.* 470, 1227. doi:10.1086/177945

Feige, J. (2014). *Supernova-produced radionuclides in deep-sea sediments measured with AMS*. Universitaet Wien: Ph.D. thesis.

Fifield, L. K., Froehlich, M., Koll, D., Pavetich, S., Slavkovská, Z., Tims, S., et al. (2022). Backgrounds and blanks in iodine-129 measurements at the Australian National University. *Nucl. Instrum. Methods Phys. Res. Sect. B Beam Interact. Mater. Atoms* 530, 8–12. doi:10.1016/j.nimb.2022.08.014

Finkel, R., and Suter, M. (1993). "AMS in the earth sciences: technique and applications," in *Advances in analytical geochemistry* (Stamford, CT: Jai Press).

Fitoussi, C., Raisbeck, G. M., Knie, K., Korschinek, G., Faestermann, T., Goriely, S., et al. (2008). Search for supernova-produced ^{60}Fe in a marine sediment. *Phys. Rev. Lett.* 101, 121101. doi:10.1103/physrevlett.101.121101

Granger, D. E. (2006). "A review of burial dating methods using ^{26}Al and ^{10}Be," in *In situ-produced cosmogenic nuclides and quantification of geological processes* (Boulder, CO: Geological Society of America). doi:10.1130/2006.2415(01)

Hain, K., Steier, P., Froehlich, M. B., Golser, R., Hou, X., Lachner, J., et al. (2020). ^{233}U/^{236}U signature allows to distinguish environmental emissions of civil nuclear industry from weapons fallout. *Nat. Commun.* 11, 1275. doi:10.1038/s41467-020-15008-2

Halbach, P. E., Jahn, A., and Cherkashov, G. (2017). *Marine Co-rich ferromanganese crust deposits: description and formation, occurrences and distribution, estimated world-wide resources.* Springer International Publishing, 65–141. doi:10.1007/978-3-319-52557-0_3

Harley, J. H. (1980). Plutonium in the environment—a review. *J. Radiat. Res.* 21, 83–104. doi:10.1269/jrr.21.83

Haynes, W. M., Lide, D. R., and Bruno, T. J. (2014). *CRC handbook of chemistry and Physics* (Boca Raton, FL: CRC Press), 95. doi:10.1201/b17118

Hein, J. R., and Koschinsky, A. (2014). "Deep-ocean ferromanganese crusts and nodules," in *Treatise on geochemistry* (Elsevier), 273–291. doi:10.1016/B978-0-08-095975-7.01111-6

Horiuchi, K., and Matsuzaki, H. (2015). Exploration of ^{10}Be analysis using 10 μg of Be carrier. *Nucl. Instrum. Methods Phys. Res. Sect. B Beam Interact. Mater. Atoms* 361, 423–430. doi:10.1016/j.nimb.2015.07.123

Hotchkis, M. A. C., Child, D., Froehlich, M., Wallner, A., Wilcken, K., and Williams, M. (2019). Actinides AMS on the VEGA accelerator. *Nucl. Instrum. Methods Phys. Res. Sect. B Beam Interact. Mater. Atoms* 438, 70–76. doi:10.1016/j.nimb.2018.07.029

Karlsson, N. B., Eisen, O., Dahl-Jensen, D., Freitag, J., Kipfstuhl, S., Lewis, C., et al. (2016). Accumulation rates during 1311–2011 CE in North-Central Greenland derived from air-borne radar data. *Front. Earth Sci.* 4. doi:10.3389/feart.2016.00097

Kelley, J. M., Bond, L. A., and Beasley, T. M. (1999). Global distribution of Pu isotopes and ^{237}Np. *Sci. Total Environ.* 237-238, 483–500. doi:10.1016/S0048-9697(99)00160-6

Ketterer, M. E., Groves, A. D., Strick, B. J., Asplund, C. S., and Jones, V. J. (2013). Deposition of ^{236}U from atmospheric nuclear testing in Washington state (USA) and the Pechora region (Russian Arctic). *J. Environ. Radioact.* 118, 143–149. doi:10.1016/j.jenvrad.2012.10.007

Ketterer, M. E., Hafer, K. M., and Mietelski, J. W. (2004). Resolving Chernobyl vs. global fallout contributions in soils from Poland using plutonium atom ratios measured by inductively coupled plasma mass spectrometry *J. Environ. Radioact.* 73, 183–201. doi:10.1016/j.jenvrad.2003.09.001

Knie, K., Korschinek, G., Faestermann, T., Dorfi, E. A., Rugel, G., and Wallner, A. (2004). ^{60}Fe anomaly in a deep-sea manganese crust and implications for a nearby supernova source. *Phys. Rev. Lett.* 93, 171103. doi:10.1103/PhysRevLett.93.171103

Knie, K., Korschinek, G., Faestermann, T., Wallner, C., Scholten, J., and Hillebrandt, W. (1999). Indication for supernova produced ^{60}Fe activity on Earth. *Phys. Rev. Lett.* 83, 18–21. doi:10.1103/physrevlett.83.18

Koll, D. (2018). *Search for recent ^{60}Fe deposition in Antarctica with AMS*. Technical University of Munich.

Koll, D. (2023). A 10-million year time profile of interstellar influx to Earth mapped through supernova ^{60}*Fe* and r-process ^{244}*Pu*. The Australian National University and Technical University Dresden. doi:10.25911/5NJB-YC98

Koll, D., Faestermann, T., Korschinek, G., Leya, I., Merchel, S., and Wallner, A. (2022a). The dyadic radionuclide system ^{60}Fe/^{53}Mn to distinguish interstellar from interplanetary ^{60}Fe. *EPJ Web Conf.* 260, 11022. doi:10.1051/epjconf/202226011022

Koll, D., Faestermann, T., Korschinek, G., and Wallner, A. (2020). Origin of recent interstellar ^{60}Fe on Earth. *EPJ Web Conf.* 232, 02001. doi:10.1051/epjconf/202023202001

Koll, D., Korschinek, G., Faestermann, T., Gómez-Guzmán, J. M., Kipfstuhl, S., Merchel, S., et al. (2019). Interstellar ^{60}Fe in Antarctica. *Phys. Rev. Lett.* 123, 072701. doi:10.1103/PhysRevLett.123.072701

Koll, D., and Lachner, J. (2023). Re-evaluation of cosmogenic ^{10}Be dating of the ferromanganese crust VA13/2 archiving interstellar radionuclides on Earth. *Res. Notes AAS* 7, 34. doi:10.3847/2515-5172/acbb75

Koll, D., Wallner, A., Battisson, S., Fichter, S., Fifield, K., Froehlich, M., et al. (2022b). Element separation chemistry and cosmogenic ^{10}Be-dating of a ferromanganese crust. *Nucl. Instrum. Methods Phys. Res. Sect. B Beam Interact. Mater. Atoms* 530, 53–58. doi:10.1016/j.nimb.2022.08.017

Korschinek, G., Bergmaier, A., Faestermann, T., Gerstmann, U., Knie, K., Rugel, G., et al. (2010). A new value for the half-life of ^{10}Be by heavy-ion elastic recoil detection and liquid scintillation counting. *Nucl. Instrum. Methods Phys. Res. Sect. B Beam Interact. Mater. Atoms* 268, 187–191. doi:10.1016/j.nimb.2009.09.020

Koschinsky, A., and Halbach, P. E. (1995). Sequential leaching of marine ferromanganese precipitates: genetic implications. *Geochimica Cosmochimica Acta* 59, 5113–5132. doi:10.1016/0016-7037(95)00358-4

Krey, P. W., and Bogen, D. C. (1987). Determination of acid leachable and total plutonium in large soil samples. *J. Radioanalytical Nucl. Chem.* 115, 335–355. doi:10.1007/BF02037448

Ku, T., Kusakabe, M., Nelson, D., Southern, J., Korteling, R., Vogel, J., et al. (1982). Constancy of oceanic deposition of ^{10}Be as recorded in manganese crusts. *Nature* 299, 240–242. doi:10.1038/299240a0

Kutschera, W., Jull, A., Paul, M., and Wallner, A. (2023). Atom counting with accelerator mass spectrometry. *Rev. Mod. Phys.* 95, 035006. doi:10.1103/revmodphys.95.035006

Lachner, J., Ploner, M., Steier, P., Sakaguchi, A., and Usui, A. (2020). Accumulation of ferromanganese crusts derived from carrier-free ^{10}Be/^{9}Be. *Nucl. Instrum. Methods Phys. Res. Sect. B Beam Interact. Mater. Atoms* 467, 146–151. doi:10.1016/j.nimb.2019.11.047

Lachner, J., Rugel, G., Vivo Vilches, C., Koll, D., Stübner, K., Winkler, S., et al. (2023). Optimization of ^{10}Be measurements at the 6MV AMS facility DREAMS. *Nucl. Instrum. Methods Phys. Res. Sect. B Beam Interact. Mater. Atoms* 535, 29–33. doi:10.1016/j.nimb.2022.11.008

Lin, M., Qiao, J., Hou, X., Dellwig, O., Steier, P., Hain, K., et al. (2021). 70-Year anthropogenic uranium imprints of nuclear activities in Baltic Sea sediments. *Environ. Sci. Technol.* 55, 8918–8927. doi:10.1021/acs.est.1c02136

Ludwig, P., Bishop, S., Egli, R., Chernenko, V., Deneva, B., Faestermann, T., et al. (2016). Time-resolved 2-million-year-old supernova activity discovered in Earth's microfossil record. *Proc. Natl. Acad. Sci.* 113, 9232–9237. doi:10.1073/pnas.1601040113

Maden, C., Döbeli, M., Kubik, P., Frank, M., and Suter, M. (2004). Measurement of carrier-free ^{10}Be samples with AMS: the method and its potential. *Nucl. Instrum. Methods Phys. Res. Sect. B Beam Interact. Mater. Atoms* 223, 247–252. doi:10.1016/j.nimb.2004.04.050

Masarik, J., and Beer, J. (1999). Simulation of particle fluxes and cosmogenic nuclide production in the Earth's atmosphere. *J. Geophys. Res. Atmos.* 104, 12099–12111. doi:10.1029/1998JD200091

Medley, B., McConnell, J. R., Neumann, T. A., Reijmer, C. H., Chellman, N., Sigl, M., et al. (2018). Temperature and snowfall in western Queen Maud Land increasing faster than climate model projections. *Geophys. Res. Lett.* 45, 1472–1480. doi:10.1002/2017GL075992

Merchel, S., Braucher, R., Lachner, J., and Rugel, G. (2021). Which is the best ^{9}Be carrier for ^{10}Be/^{9}Be accelerator mass spectrometry? *MethodsX* 8, 101486. doi:10.1016/j.mex.2021.101486

Merchel, S., and Herpers, U. (1999). An update on radiochemical separation techniques for the determination of long-lived radionuclides via accelerator mass spectrometry. *Radiochim. Acta* 84, 215–220. doi:10.1524/ract.1999.84.4.215

Muramatsu, Y., Rühm, W., Yoshida, S., Tagami, K., Uchida, S., and Wirth, E. (2000). Concentrations of ^{239}Pu and ^{240}Pu and their isotopic ratios determined by ICP-MS in soils collected from the Chernobyl 30-km zone. *Environ. Sci. Technol.* 34, 2913–2917. doi:10.1021/es0008968

Nagai, H., Tada, W., and Kobayashi, T. (2000). Production rates of ^{7}Be and ^{10}Be in the atmosphere. *Nucl. Instrum. Methods Phys. Res. Sect. B Beam Interact. Mater. Atoms* 172, 796–801. doi:10.1016/S0168-583X(00)00124-5

NEA/OECD (2002). *Chernobyl - assessment of radiological and health impacts*.

Nishiizumi, K., Lal, D., Klein, J., Middleton, R., and Arnold, J. (1986). Production of ^{10}Be and ^{26}Al by cosmic rays in terrestrial quartz *in situ* and implications for erosion rates. *Nature* 319, 134–136. doi:10.1038/319134a0

Ochs, M., and Ivy-Ochs, S. (1997). The chemical behavior of Be, Al, Fe, Ca and Mg during AMS target preparation from terrestrial silicates modeled with chemical speciation calculations. *Nucl. Instrum. Methods Phys. Res. Sect. B Beam Interact. Mater. Atoms* 123, 235–240. doi:10.1016/s0168-583x(96)00680-5

Oerter, H., Wilhelms, F., Jung-Rothenhäusler, F., Göktas, F., Miller, H., Graf, W., et al. (2000). Accumulation rates in Dronning Maud Land, Antarctica, as revealed by dielectric-profiling measurements of shallow firn cores. *Ann. Glaciol.* 30, 27–34. doi:10.3189/172756400781820705

Onda, Y., Taniguchi, K., Yoshimura, K., Kato, H., Takahashi, J., Wakiyama, Y., et al. (2020). Radionuclides from the Fukushima Daiichi nuclear power plant in terrestrial systems. *Nat. Rev. Earth Environ.* 1, 644–660. doi:10.1038/s43017-020-0099-x

Qiao, J., Ransby, D., and Steier, P. (2022). Deciphering anthropogenic uranium sources in the equatorial northwest Pacific margin. *Sci. Total Environ.* 806, 150482. doi:10.1016/j.scitotenv.2021.150482

Rugel, G., Faestermann, T., Knie, K., Korschinek, G., Poutivtsev, M., Schumann, D., et al. (2009). New measurement of the ^{60}Fe half-life. *Phys. Rev. Lett.* 103, 072502. doi:10.1103/PhysRevLett.103.072502

Rugel, G., Pavetich, S., Akhmadaliev, S., Enamorado Baez, S. M., Scharf, A., Ziegenrücker, R., et al. (2016). The first four years of the AMS-facility DREAMS: status and developments for more accurate radionuclide data. *Nucl. Instrum. Methods Phys. Res. Sect. B Beam Interact. Mater. Atoms* 370, 94–100. doi:10.1016/j.nimb.2016.01.012

Segl, M., Mangini, A., Bonani, G., Hofmann, H., Nessi, M., Suter, M., et al. (1984). ^{10}Be-dating of a manganese crust from central North Pacific and implications for ocean palaeocirculation. *Nature* 309, 540–543. doi:10.1038/309540a0

Smith, T., Cook, D. L., Merchel, S., Pavetich, S., Rugel, G., Scharf, A., et al. (2019). The constancy of galactic cosmic rays as recorded by cosmogenic nuclides in iron meteorites. *Meteorit. Planet. Sci.* 54, 2951–2976. doi:10.1111/maps.13417

Steier, P., Hain, K., Klötzli, U., Lachner, J., Priller, A., Winkler, S., et al. (2019). The actinide beamline at VERA. *Nucl. Instrum. Methods Phys. Res. Sect. B Beam Interact. Mater. Atoms* 458, 82–89. doi:10.1016/j.nimb.2019.07.031

Steier, P., Hrnecek, E., Priller, A., Quinto, F., Srncik, M., Wallner, A., et al. (2013). AMS of the minor plutonium isotopes. *Nucl. Instrum. Methods Phys. Res. Sect. B Beam Interact. Mater. Atoms* 294, 160–164. doi:10.1016/j.nimb.2012.06.017

Synal, H.-A. (2013). Developments in accelerator mass spectrometry. *Int. J. Mass Spectrom.* 349-350, 192–202. doi:10.1016/j.ijms.2013.05.008

Synal, H.-A. (2022). Accelerator mass spectrometry: ultra-sensitive detection technique of long-lived radionuclides. *Chimia* 76, 45–51. doi:10.2533/chimia.2022.45

Tighe, C., Castrillejo, M., Christl, M., Degueldre, C., Andrew, J., Semple, K. T., et al. (2021). Local and global trace plutonium contributions in fast breeder legacy soils. *Nat. Commun.* 12, 1381. doi:10.1038/s41467-021-21575-9

UNSCEAR (2000). "Sources and effects of ionizing radiation," in *United nations scientific committee on the effects of atomic radiation (UNSCEAR) 2000 report*. doi:10.18356/49c437f9-en

UNSCEAR (2010). UNSCEAR 2008 - sources and effects of ionizing radiation. *Report*. doi:10.18356/cb7b6e26-en

Vivo-Vilches, C., Rugel, G., Lachner, J., Koll, D., Stübner, K., Fichter, S., et al. (2023). Pushing the limits of ^{41}Ca AMS with CaF_2 targets at DREAMS. *Nucl. Instrum. Methods Phys. Res. Sect. B Beam Interact. Mater. Atoms* 540, 188–193. doi:10.1016/j.nimb.2023.04.050

Vockenhuber, C., Alfimov, V., Christl, M., Lachner, J., Schulze-König, T., Suter, M., et al. (2013). The potential of He stripping in heavy ion AMS. *Nucl. Instrum. Methods Phys. Res. Sect. B* 294, 382–386. doi:10.1016/j.nimb.2012.01.014

von Blanckenburg, F., Belshaw, N., and O'Nions, R. (1996a). Separation of ^{9}Be and cosmogenic ^{10}Be from environmental materials and SIMS isotope dilution analysis. *Chem. Geol.* 129, 93–99. doi:10.1016/0009-2541(95)00157-3

von Blanckenburg, F., O'Nions, R., Belshaw, N., Gibb, A., and Hein, J. (1996b). Global distribution of beryllium isotopes in deep ocean water as derived from Fe-Mn crusts. *Earth Planet. Sci. Lett.* 141, 213–226. doi:10.1016/0012-821x(96)00059-3

Wallner, A., Bichler, M., Buczak, K., Dressler, R., Fifield, L. K., Schumann, D., et al. (2015). Settling the half-life of ^{60}Fe: fundamental for a versatile astrophysical chronometer. *Phys. Rev. Lett.* 114, 041101. doi:10.1103/PhysRevLett.114.041101

Wallner, A., Feige, J., Fifield, L. K., Froehlich, M. B., Golser, R., Hotchkis, M. A. C., et al. (2020). ^{60}Fe deposition during the late Pleistocene and the Holocene echoes past supernova activity. *Proc. Natl. Acad. Sci.* 117, 21873–21879. doi:10.1073/pnas.1916769117

Wallner, A., Feige, J., Kinoshita, N., Paul, M., Fifield, L., Golser, R., et al. (2016). Recent near-Earth supernovae probed by global deposition of interstellar radioactive ^{60}Fe. *Nature* 532, 69–72. doi:10.1038/nature17196

Wallner, A., Fifield, L., Froehlich, M., Koll, D., Leckenby, G., Martschini, M., et al. (2023). Accelerator mass spectrometry with ANU's 14 million volt accelerator. *Nucl. Instrum. Methods Phys. Res. Sect. B Beam Interact. Mater. Atoms* 534, 48–53. doi:10.1016/j.nimb.2022.10.021

Wallner, A., Froehlich, M. B., Hotchkis, M. A. C., Kinoshita, N., Paul, M., Martschini, M., et al. (2021). ^{60}Fe and ^{244}Pu deposited on Earth constrain the r-process yields of recent nearby supernovae. *Science* 372, 742–745. doi:10.1126/science.aax3972

Webber, W. R., and Higbie, P. R. (2003). Production of cosmogenic Be nuclei in the Earth's atmosphere by cosmic rays: its dependence on solar modulation and the interstellar cosmic ray spectrum. *J. Geophys. Res. Space Phys.* 108. doi:10.1029/2003JA009863

Wilcken, K., Hotchkis, M., Levchenko, V., Fink, D., Hauser, T., and Kitchen, R. (2015). From carbon to actinides: a new universal 1MV accelerator mass spectrometer at ANSTO. *Nucl. Instrum. Methods Phys. Res. Sect. B Beam Interact. Mater. Atoms* 361, 133–138. doi:10.1016/j.nimb.2015.04.054

Xiao, C., Du, Z., Handley, M. J., Mayewski, P. A., Cao, J., Schüpbach, S., et al. (2020). Iron in the NEEM ice core relative to Asian loess records over the last glacial–interglacial cycle. *Natl. Sci. Rev.* 8, nwaa144. doi:10.1093/nsr/nwaa144